



SUBSURFACE CHARACTERIZATION OF 67P/CHURYUMOV–GERASIMENKO’S ABYDOS SITE

B. BRUGGER¹, O. MOUSIS¹, A. MORSE², U. MARBOEUF³, L. JORDA¹, A. GUILBERT-LEPOUTRE⁴, D. ANDREWS², S. BARBER², P. LAMY¹, A. LUSPAY-KUTI⁵, K. MANDT⁵, G. MORGAN², S. SHERIDAN², P. VERNAZZA¹, AND I. P. WRIGHT²

¹ Aix Marseille Université, CNRS, LAM (Laboratoire d’Astrophysique de Marseille) UMR 7326, F-13388, Marseille, France; bastien.brugger@lam.fr

² Planetary and Space Sciences, Department of Physics, The Open University, Walton Hall, Milton Keynes MK7 6AA, UK

³ Physikalisches Institut, Center for Space and Habitability, University of Bern, Switzerland

⁴ Institut UTINAM, UMR 6213 CNRS-Université de Franche-Comté, Besançon, France

⁵ Department of Space Science, Southwest Research Institute, 6220 Culebra Road, San Antonio, TX 78228, USA

Received 2015 November 3; accepted 2016 March 15; published 2016 May 11

ABSTRACT

On 2014 November 12, the ESA/*Rosetta* descent module *Philae* landed on the Abydos site of comet 67P/Churyumov–Gerasimenko. Aboard this module, the Ptolemy mass spectrometer measured a CO/CO₂ ratio of 0.07 ± 0.04, which differs substantially from the value obtained in the coma by the *Rosetta*/ROSINA instrument, suggesting a heterogeneity in the comet nucleus. To understand this difference, we investigated the physicochemical properties of the Abydos subsurface, leading to CO/CO₂ ratios close to that observed by Ptolemy at the surface of this region. We used a comet nucleus model that takes into account different water ice phase changes (amorphous ice, crystalline ice, and clathrates) as well as diffusion of molecules throughout the pores of the matrix. The input parameters of the model were optimized for the Abydos site, and the ROSINA CO/CO₂ measured ratio is assumed to correspond to the bulk value in the nucleus. We find that all considered structures of water ice are able to reproduce the Ptolemy observation with a time difference not exceeding ~50 days, i.e., lower than ~2% on 67P/Churyumov–Gerasimenko’s orbital period. The suspected heterogeneity of 67P/Churyumov–Gerasimenko’s nucleus is also found possible only if it is constituted of crystalline ices. If the icy phase is made of amorphous ice or clathrates, the difference between Ptolemy and ROSINA’s measurements would rather originate from the spatial variations in illumination on the nucleus surface. An eventual new measurement of the CO/CO₂ ratio at Abydos by Ptolemy could be decisive to distinguish between the three water ice structures.

Key words: comets: general – comets: individual (67P/Churyumov–Gerasimenko) – methods: numerical – solid state: volatile

1. INTRODUCTION

On 2014 November 12, the ESA/*Rosetta* descent module *Philae* landed at the Abydos site on the surface of comet 67P/Churyumov–Gerasimenko (hereafter 67P/C-G). As part of the scientific payload aboard *Philae*, the Ptolemy mass spectrometer (Wright et al. 2007) performed the analysis of several samples from the surface at Agilkia (Wright et al. 2015) and atmosphere at Abydos (Morse et al. 2015). The main molecules detected by Ptolemy on the Abydos site were H₂O, CO, and CO₂, with a measured CO/CO₂ molar ratio of 0.07 ± 0.04. Meanwhile, the CO/CO₂ ratio has also been sampled in 67P/C-G’s coma between 2014 August and September by the ROSINA Double Focusing Mass Spectrometer (DFMS; Balsiger et al. 2007; Hässig et al. 2013) aboard the *Rosetta* spacecraft. Strong variations of the CO and CO₂ production rates, dominated by the diurnal changes on the comet, have been measured by ROSINA, giving CO/CO₂ ratios ranging between 0.50 ± 0.18 and 1.62 ± 1.34 over the 2014 August–September time period (Hässig et al. 2015). Large fluctuations correlated with the sampled latitudes have also been observed and explained either by seasonal variations or by a compositional heterogeneity in the nucleus (Hässig et al. 2015). Further investigation of the coma heterogeneity performed by Luspay-Kuti et al. (2015) in the southern hemisphere of 67P/C-G at a later time period led to conclusions in favor of compositional heterogeneity. The latter hypothesis is also reinforced by the Ptolemy measurement of the CO/CO₂ ratio at the Abydos site, which is found outside the range covered by the ROSINA measurements (Morse et al. 2015).

Here we aim at investigating the physicochemical properties of the Abydos subsurface that can reproduce the CO/CO₂ ratio observed by Ptolemy, assuming that the composition of the solid phase located beneath the landing site initially corresponds to the value in the coma. To investigate the possibility of a heterogeneous nucleus for 67P/C-G, we have employed a comet nucleus model with (i) an updated set of thermodynamic parameters relevant for this comet and (ii) an appropriate parameterization of the illumination at the Abydos site. This allows us to mimic the thermal evolution of the subsurface of this location. By searching for the matching conditions between the properties of the Abydos subsurface and the Ptolemy data, we provide several constraints on the structural properties and composition of *Philae*’s landing site in different cases.

2. THE COMET NUCLEUS MODEL

The one-dimensional comet nucleus model used in this work is described in Marboeuf et al. (2012). This model considers an initially homogeneous sphere composed of a predefined porous mixture of ices and dust in specified proportions. It describes heat transmission, gas diffusion, sublimation/recondensation of volatiles within the nucleus, water ice phase transition, dust release, and dust mantle formation. The model takes into account different phase changes of water ice, within amorphous ice, crystalline ice, and clathrates. The use of a 1D model is a good approximation for the study of a specific point at the surface of the comet nucleus, here the Abydos landing site. However, since 67P/C-G’s shape is far from being a sphere (Sierks et al. 2015), we have parameterized the model in a way

Table 1
Modeling Parameters for the Nucleus

Parameter	Value	Reference
Rotation period (hr)	12.4	Mottola et al. (2014)
Obliquity (deg)	52.25	...
Subsolar meridian Φ (deg) ^a	-111	...
Co-latitude (deg) ^b	-21	...
Initial radius (km)	2.43	...
Bolometric albedo (%)	1.5	Fornasier et al. (2015)
Dust/ice mass ratio	4 ± 2	Rotundi et al. (2014)
Porosity (%)	80 ± 5	Kofman et al. (2015)
Density (kg m^{-3})	510 ± 20	Jorda et al. (2014)
I ($\text{W K}^{-1} \text{m}^{-2} \text{s}^{1/2}$) ^c	50	Leyrat et al. (2015)
CO/CO ₂ initial ratio	1.62 ± 1.34	Hässig et al. (2015)

Notes.

^a Argument of subsolar meridian at perihelion.

^b Angle between the normal to the surface and the equatorial plane.

^c Thermal inertia.

that correctly reproduces the illumination conditions at Abydos. This has been made possible via the use of the 3D shape model developed by Jorda et al. (2014), which gives the coordinates of Abydos on the surface of 67P/C-G's nucleus, as well as the radius corresponding to the Abydos landing site and the normal to the surface at this specific location. The Abydos landing site is located just outside the Hatmethit depression, at the very edge of the area illuminated during the mapping and close observation phases of the *Rosetta* mission, roughly until 2014 December. It is also at the edge of a relatively flat region of the small lobe illuminated throughout the perihelion passage of the comet. Geomorphologically, Abydos is interpreted as being a rough deposit region composed of meter-sized boulders (Lucchetti et al. 2016). Other geometric parameters specific to 67P/C-G, such as the obliquity and the argument of the subsolar meridian at perihelion, are calculated from the orientation of the spin axis computed during the shape reconstruction process (Jorda et al. 2014). Table 1 summarizes the main parameters used in this work. The porosity and dust/ice ratio of the cometary material are set in the range of measurement of $80\% \pm 5\%$ (Kofman et al. 2015) and 4 ± 2 (Rotundi et al. 2014), respectively. These two parameters are linked through the density of the cometary material and are set to be compatible with the preliminary value determined by Jorda et al. (2014) ($510 \pm 20 \text{ kg m}^{-3}$). 67P/C-G's thermal inertia is estimated to be in the $10\text{--}150 \text{ W K}^{-1} \text{ m}^{-2} \text{ s}^{1/2}$ range based on the measurement obtained by the *Rosetta*/VIRTIS instrument (Leyrat et al. 2015). According to the same study, regions surrounding Abydos are characterized by a thermal inertia in the lower half of this range. We have therefore chosen a low thermal inertia close to $50 \text{ W K}^{-1} \text{ m}^{-2} \text{ s}^{1/2}$.

In addition to water ice and dust, the solid phase of our model includes CO and CO₂ volatiles. Although coma abundances do not necessarily reflect those in the nucleus, they constitute the most relevant constraint available on its composition. We thus considered the CO/CO₂ ratio (1.62 ± 1.34) measured by ROSINA on 2014 August 7 at 18 hr, as representative of the bulk ice composition in the nucleus, and more specifically in the Abydos subsurface. This ratio is derived from the CO/H₂O and CO₂/H₂O ROSINA measurements performed at this date, which are equal to 0.13 ± 0.07 and 0.08 ± 0.05 , respectively (Hässig et al. 2015). We

selected the date of August 7 because (i) the corresponding ROSINA measurements were performed at high northern latitudes where the Abydos site is located, and (ii) the large CO/CO₂ range obtained at this moment covers all values measured by ROSINA at other dates (including the late value obtained by Le Roy et al. [2015] on October 20 for the northern hemisphere, namely, $\text{CO}/\text{CO}_2 = 1.08$).

The three main phases of ices identified in the literature, namely, crystalline ice, amorphous ice, and clathrate phase, are considered in this work. Outgassing of volatiles in 67P/C-G could then result from the sublimation of ices, amorphous-to-crystalline ice phase transition, or destabilization of clathrates in the crystalline ice, amorphous ice, and clathrates cases, respectively. Because the properties of volatiles trapping in the nucleus matrix strongly depend on the considered icy phase, the following models have been considered:

Crystalline ice model. Water ice is fully crystalline, meaning that no volatile species are trapped in the water ice structure. Here CO and CO₂ are condensed in the pores of the matrix made of water ice and dust.

Amorphous ice model. The matrix itself is made of amorphous water ice with a volatile trapping efficiency not exceeding $\sim 10\%$. In this case, the cumulated mole fraction of volatiles is higher than this value, implying that an extra amount of volatiles is crystallized in the pores. With this in mind, we consider different distributions of CO and CO₂ in both phases of this model.

Clathrate model. Water ice is exclusively used to form clathrates. Similarly to amorphous ice, clathrates have a maximum trapping capacity ($\sim 17\%$). The extra amount of volatiles, if any, also crystallizes in the pores. In our case, however, CO is fully trapped in clathrates and escapes only when water ice sublimates. In contrast, we assume that solid CO₂ exists in the form of crystalline CO₂ in the pores of the nucleus because this molecule is expected to condense in this form in the protosolar nebula (Mousis et al. 2008).

3. THERMAL EVOLUTION OF THE SUBSURFACE AT ABYDOS

Our results show that the illumination at the surface of the Abydos site is a critical parameter for the evolution of the nucleus, regardless of the considered ice structure. Consequently, all three models described in Section 2 present the same behavior up to a given point. We first describe the characteristics displayed in common by the three models by presenting the thermal evolution of the crystalline ice model, before discussing the variations resulting from the different assumptions on the nature of ices. Figure 1 shows the time evolution of the nucleus stratigraphy, which corresponds to the structural differentiation occurring in the subsurface of the Abydos site. This differentiation results from the sublimation of the different ices. After each perihelion passage, the sublimation interfaces of CO and CO₂ reach deeper layers beneath the nucleus surface, with a progression of ~ 20 m per orbit. The CO sublimation interface always propagates deeper than its CO₂ counterpart because of the higher volatility of the former molecule. On the other hand, because surface ablation is significant, the progression of these interfaces is stopped by the propagation of the water sublimation front after perihelion. This allows the Abydos region to present a “fresh” surface after each perihelion.

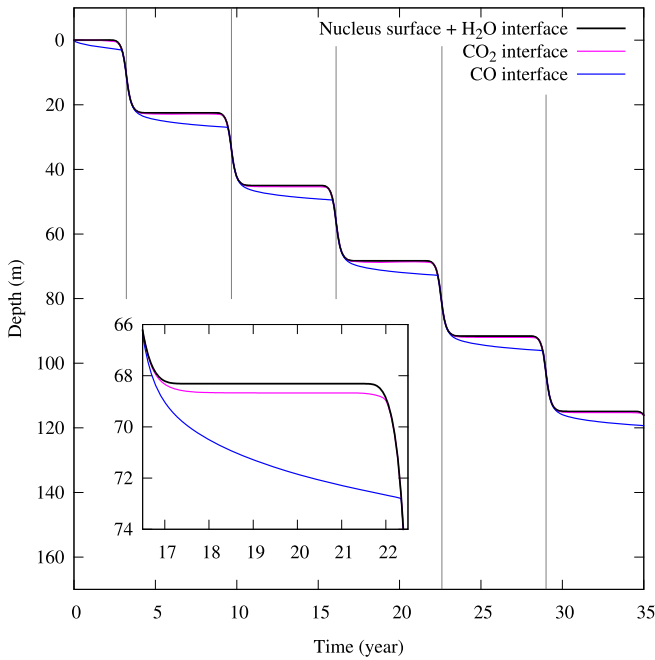


Figure 1. Stratigraphy of the Abydos subsurface represented during 35 yr of evolution (~ 5 orbits of 67P/C-G), showing the interfaces of sublimation of considered volatile species. The surface ablation occurs at each perihelion (represented by the vertical lines) and reaches all interfaces.

At the surface of the Abydos site, the outgassing rates of CO and CO₂ vary with the illumination conditions, reaching maxima at perihelion and minima at aphelion. Because the sublimation interface of CO₂ is closer to the surface, its production rate is more sensitive to the illumination conditions than that of CO. As a result, the outgassing rate of CO₂ presents important variations with illumination, while that of CO is less affected. This difference strongly impacts the evolution of the CO/CO₂ outgassing ratio at the surface of Abydos (see Figure 2). Close to perihelion, this ratio crosses the range of values measured by Ptolemy (0.07 ± 0.04) and reaches a minimum. Note that the CO/CO₂ outgassing ratio presents spikes during a certain period after perihelion. These spikes appear when the CO and CO₂ interfaces of sublimation are dragged out to the surface by ablation and result from temperature variations induced by diurnal variations of the insolation.

We define Δt as the time difference existing between the Ptolemy CO/CO₂ observations (here 0.07 measured on 2014 November 12) and the epoch at which our model reproduces these data (see Figure 2). In each case investigated, we vary the input parameters of the model to minimize the value of Δt (see Table 2 for details). We have also defined the quantity $f_i = \Delta t/P_{\text{orb}}$, namely, the fraction of 67P/C-G’s orbital period ($P_{\text{orb}} = 6.44$ yr) corresponding to Δt . The results of our simulations are indicated below.

Crystalline ice model. In this case, we find that the initial CO/CO₂ ratio and the dust/ice ratio adopted in the nucleus have a strong influence on Δt . This quantity is minimized (i) when the adopted dust/ice ratio becomes higher than those found by Rotundi et al. (2014) and (ii) if the selected initial CO/CO₂ ratio is lower than the nominal value found by ROSINA (Hässig et al. 2015). Figure 3 shows the evolution of Δt as a function of the dust/ice ratio for two different values of the initial CO/CO₂ ratio, namely, 1.62 (the central value) and

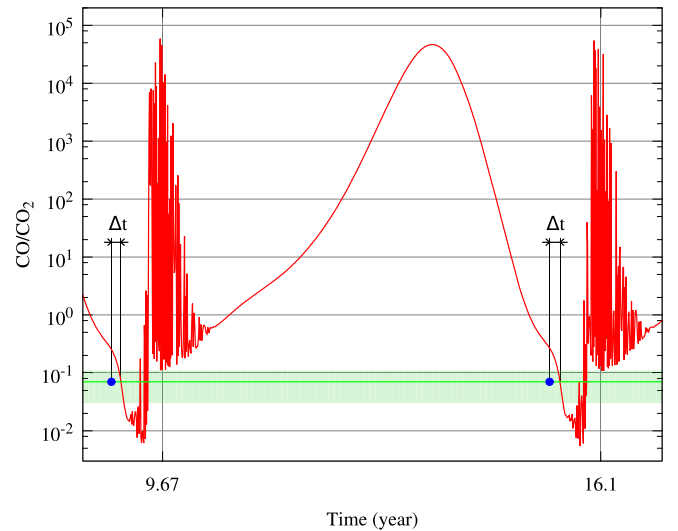


Figure 2. Evolution of the CO/CO₂ outgassing ratio at Abydos in the case of the crystalline ice model, during one orbit. The green line and green area represent the Ptolemy central value and its range of uncertainty, respectively. The blue dots correspond to the measurement epoch (2014 November 12). Vertical lines correspond to passages at perihelion. See text for a description of Δt .

Table 2
Optimized Set of Parameters for the Three Models

	Crystalline Ice Model	Amorphous Ice Model	Clathrate Model
Parameters			
Dust/ice mass ratio	6	4	4
Porosity (%)	78	76	76
Density (kg m ⁻³)	516	510	519
I (W K ⁻¹ m ⁻² s ^{1/2}) ^a	~ 60	40–60	~ 50
CO/CO ₂ initial ratio	0.46	1.62	0.46
CO/H ₂ O initial abundance	6%	13% ^b	6%
CO ₂ /H ₂ O initial abundance	13	8% ^c	13%
Results			
Δt (days)	52	4	34
f_i (%)	2.2	0.17	1.4

Notes.

^a Thermal inertia resulting from the different water ice conductivities.

^b 2.8% trapped in amorphous ice, 10.2% condensed in the pores (Marboeuf et al. 2012).

^c 4.2% trapped in amorphous ice, 3.2% condensed in the pores (Marboeuf et al. 2012).

0.46 (close to the lower limit). These results confirm the aforementioned trend: with CO/CO₂ = 0.46 and a dust/ice ratio of 6 or higher, Ptolemy’s measurement epoch is matched with $\Delta t = 52 \pm 27$ days or lower, which corresponds to f_i lower than $\sim 2\%$. These results can be explained by the thermal conductivity of crystalline water ice, which is in the 3–20 W m⁻¹ K⁻¹ range (Klinger 1980), considering the temperatures in the comet. Because dust has a conductivity of 4 W m⁻¹ K⁻¹ (Ellsworth & Schubert 1983), the global conductivity decreases with the increase of the dust/ice ratio in the nucleus. Since

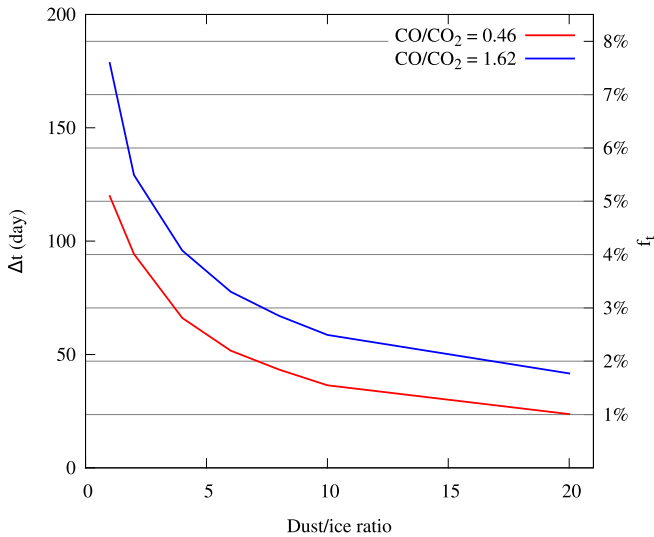


Figure 3. Evolution of Δt and f_i as a function of the dust/ice mass ratio for two different values of the initial CO/CO_2 ratio in the case of the crystalline ice model (see text).

heating in the nucleus is mostly provided by surface illumination, a low conductivity increases the temperature gradient between the upper and deeper layers (where the CO_2 and the CO sublimation interfaces are located, respectively). This gradient enhances more the sublimation rate of CO_2 ice than that of CO ice, leading to smaller CO/CO_2 outgassing ratios at the surface and to a smaller Δt (see Figure 2).

Amorphous ice model. Here values of Δt are significantly lower than those obtained with the crystalline ice model; a Δt of 4 ± 9 days is obtained using the central values listed in Table 2 for the initial CO/CO_2 and dust/ice ratios, leading to $f_i \sim 0.2\%$. Higher values of the CO/CO_2 ratio never allow our model to match the Ptolemy data: the CO/CO_2 outgassing ratio is increased sufficiently high so that even its minimum becomes higher than the range of measurements performed by Ptolemy. On the other hand, lower CO/CO_2 ratios increase Δt . Interestingly, the results of this model are poorly affected by the considered dust/ice ratio. Within the $0.12\text{--}1.35 \text{ W m}^{-1} \text{ K}^{-1}$ range (Klinger 1980), the conductivity of amorphous water ice lies under those of dust ($4 \text{ W m}^{-1} \text{ K}^{-1}$) and crystalline ices ($3\text{--}20 \text{ W m}^{-1} \text{ K}^{-1}$). Since amorphous ice dominates the volatile phase, the mean conductivity is never too far from that of dust, irrespective of the dust/ice ratio considered within the observed range.

Clathrate model. In this case, low CO/CO_2 ratios (still within the range given in Table 1) are required to get values of Δt below 50 days (i.e., f_i below 2%). Similarly to the case of the amorphous ice model, Δt is poorly sensitive to the variation of the dust/ice ratio because the conductivity of clathrates ($0.5 \text{ W m}^{-1} \text{ K}^{-1}$; Krivchikov et al. 2005a, 2005b) is small compared with that of dust.

4. DISCUSSION

Our goal was to investigate the possibility of recovering the value of the CO/CO_2 outgassing ratio measured by the Ptolemy instrument at the surface of Abydos. Interestingly, all considered models match the Ptolemy value with f_i lower than $\sim 2\%$, provided that an optimized set of parameters is adopted for the Abydos region. Despite the fact that it is poorly

sensitive to the adopted dust/ice ratio, a nucleus model dominated by amorphous ice (and possibly including a smaller fraction of crystalline ices) gives the best results ($\Delta t \leq 4$ days, i.e., $f_i \leq 0.2\%$) for a primordial CO/CO_2 ratio equal to the central value measured by the ROSINA instrument. On the other hand, the crystalline ice and clathrate models require a primordial CO/CO_2 ratio close to the lower limit sampled by ROSINA to obtain values of Δt under 50 days (i.e., f_i under 2%). We stress the fact that the CO/CO_2 range of validity is used under the assumption that the ROSINA measurements correspond to the bulk nucleus abundances, which is not necessarily true. A second requirement to minimize the value of Δt in the crystalline ice model is the necessity to adopt a dust/ice ratio at least equal to or higher than the upper limit determined by Rotundi et al. (2014) for 67P/C-G. This is supported by the pictures taken at Abydos by the CIVA instrument (Bibring et al. 2007) aboard the *Philae* module. The very low reflectance of 3%–5% of the Abydos region (Bibring et al. 2015) is in agreement with the OSIRIS and VIRTIS reflectance measurements in the visible (Sierks et al. 2015) and near-IR (Capaccioni et al. 2015), which are consistent with a low ice content in the upper surface layer (Capaccioni et al. 2015).

Surface illumination can also greatly influence the CO/CO_2 outgassing ratio on 67P/C-G. To quantify this effect, we have simulated a point of 67P/C-G’s nucleus, which is more illuminated in comparison to Abydos. We have performed a set of simulations at a co-latitude of -52.25° , a point that receives permanent sunlight around perihelion. At the date when the CO/CO_2 outgassing ratio at Abydos is equal to 0.07 (the central value of Ptolemy’s range of measurement), we obtain a different value for the CO/CO_2 outgassing ratio at this new location, irrespective of the adopted model. For the crystalline ice model, the outgassing ratio at the illuminated site reaches a value of 0.11, which is still within Ptolemy’s range of measurement. This implies that a different illumination cannot explain a strong variation of the CO/CO_2 outgassing ratio if the nucleus presents a homogeneous composition. In this case, the difference between the Ptolemy and ROSINA measurements is clearly due to a heterogeneity in the nucleus composition. On the other hand, the CO/CO_2 outgassing ratio at the illuminated site is equal to 0.74 and 0.76 in the cases of the amorphous ice and clathrate models, respectively. These values are within ROSINA’s range of measurements, implying that the difference of illumination is sufficient to explain the difference with the CO/CO_2 ratio sampled at Abydos, assuming a homogeneous nucleus.

In summary, all possible water ice structures are able to reproduce the observations made by Ptolemy, assuming that the primordial CO/CO_2 ratio is the one inferred by ROSINA. Each case requires a unique set of input parameters taken from the range of values inferred by *Rosetta* and which describes the structure and composition of the material. According to our simulations, a heterogeneity in the composition of 67P/C-G’s nucleus is possible only if the nucleus is composed of crystalline ices. However, if we consider different ice phases like amorphous ice or clathrates, the difference between the Ptolemy and ROSINA measurements could simply originate from the variation of illumination between different regions of the nucleus.

In the upcoming months, the *Philae* module could awaken and allow the Ptolemy mass spectrometer to perform additional

measurements of the CO/CO₂ ratio. By comparing these new values with the different CO/CO₂ outgassing ratios predicted by our three models at the same date, we would be able to see which model is the most reliable and thus to determine which water ice structure is dominant at the surface of 67P/C-G's nucleus.

O.M. acknowledges support from CNES. This work has been partly carried out thanks to the support of the A*MIDEX project (n° ANR-11-IDEX-0001-02) funded by the “Investissements d’Avenir” French government program, managed by the French National Research Agency (ANR). Funding and operation of the Ptolemy instrument was provided by the Science and Technology Facilities Council (consolidated grant ST/L000776/1) and UK Space Agency (Post-launch support ST/K001973/1). A.L.-K. acknowledges support from the NASA Jet Propulsion Laboratory (subcontract no. 1496541).

REFERENCES

- Balsiger, H., Altwegg, K., Bochsler, P., et al. 2007, *SSRv*, **128**, 745
 Bibring, J.-P., Lamy, P., Langevin, Y., et al. 2007, *SSRv*, **128**, 397
 Bibring, J.-P., Langevin, Y., Carter, J., et al. 2015, *Sci*, **349**, 020671
 Capaccioni, F., Coradini, A., Filacchione, G., et al. 2015, *Sci*, **347**, 0628
 Ellsworth, K., & Schubert, G. 1983, *Icar*, **54**, 490
 Fornasier, S., Hasselmann, P. H., Barucci, M. A., et al. 2015, *A&A*, **583**, A30
 Hässig, M., Altwegg, K., Balsiger, H., et al. 2013, *P&SS*, **84**, 148
 Hässig, M., Altwegg, K., Balsiger, H., et al. 2015, *Sci*, **347**, 276
 Jorda, L., Gaskell, R. W., Hviid, S. F., et al. 2014, *AGUFM*, **3943**
 Klinger, J. 1980, *Sci*, **209**, 271
 Kofman, W., Herique, A., Barbin, Y., et al. 2015, *Sci*, **349**, 020639
 Krivchikov, A. I., Gorodilov, B. Y., Korolyuk, O. A., et al. 2005a, *JLTP*, **139**, 693
 Krivchikov, A. I., Manzhelii, V. G., Korolyuk, O. A., Gorodilov, B. Y., & Romantsova, O. O. 2005b, *PCCP*, **7**, 728
 Le Roy, L., Altwegg, K., Balsiger, H., et al. 2015, *A&A*, **583**, A1
 Leyrat, C., Erard, S., Capaccioni, F., et al. 2015, EGU General Assembly Conference Abstracts, **17**, 9767
 Lucchetti, A., Cremonese, G., Jorda, L., et al. 2016, *A&A*, **585**, L1
 Luspay-Kuti, A., Hässig, M., Fuselier, S. A., et al. 2015, *A&A*, **583**, A4
 Marboeuf, U., Schmitt, B., Petit, J.-M., Mouis, O., & Fray, N. 2012, *A&A*, **542**, A82
 Morse, A., Mouis, O., Sheridan, S., et al. 2015, *A&A*, **583**, A42
 Mottola, S., Lowry, S., Snodgrass, C., et al. 2014, *A&A*, **569**, L2
 Mouis, O., Alibert, Y., Hestroffer, D., et al. 2008, *MNRAS*, **383**, 1269
 Rotundi, A., Rietmeijer, F. J. M., Ferrari, M., et al. 2014, *M&PS*, **49**, 550
 Sierks, H., Barbieri, C., Lamy, P. L., et al. 2015, *Sci*, **347**, 1044
 Wright, I. P., Barber, S. J., Morgan, G. H., et al. 2007, *SSRv*, **128**, 363
 Wright, I. P., Sheridan, S., Barber, S. J., et al. 2015, *Sci*, **349**, 020673